

# Measurement of the current-phase relation of superconductor/ferromagnet/superconductor $\pi$ Josephson junctions

S. M. Frolov and D. J. Van Harlingen

*Department of Physics, University of Illinois at Urbana-Champaign, Urbana, Illinois 61801, USA*

V. A. Oboznov, V. V. Bolginov, and V. V. Ryazanov

*Institute of Solid State Physics, Russian Academy of Sciences, Chernogolovka, 142432, Russia*

(Received 1 June 2004; published 13 October 2004)

We present measurements of the current-phase relation (CPR) of superconductor-ferromagnet-superconductor (SFS) Josephson junctions as a function of temperature. The CPR is determined by incorporating the junction into a superconducting loop coupled to a dc SQUID, allowing measurement of the junction phase difference. We find that the critical current of Nb-Cu<sub>0.47</sub>Ni<sub>0.53</sub>-Nb Josephson junctions with barrier thickness  $\sim 22$  nm changes sign at  $T < T_\pi \sim 2-4$  K, indicating that the junction becomes a  $\pi$  Josephson junction. We find no evidence for second-order Josephson tunneling near  $T_\pi$  in the CPR predicted by several theories.

DOI: 10.1103/PhysRevB.70.144505

PACS number(s): 74.50.+r

The interplay between superconductivity and magnetism in thin film superconductor-ferromagnetic (SF) structures has long attracted substantial theoretical and experimental attention. Over 20 years ago, it was predicted that a superconductor-ferromagnet-superconductor (SFS) Josephson junction could become a  $\pi$  junction, characterized by a minimum Josephson coupling energy at a phase difference of  $\pi$ , due to exchange field-induced oscillations of the order parameter (OP) in the ferromagnetic barrier.<sup>1</sup> Such  $\pi$  junctions were only achieved recently in systems with weak ferromagnetic barriers and demonstrated by conventional transport<sup>2-6</sup> and SQUID interference<sup>7-9</sup> measurements.  $\pi$  Josephson behavior has also been reported in mesoscopic superconductor-normal metal-superconductor (SNS) junctions driven into a nonequilibrium state by the injection of quasiparticles into the barrier,<sup>10,11</sup> in submicron cuprate grain boundary junctions for which the supercurrent is dominated by zero-energy Andreev bound states induced by the  $d$ -wave order parameter,<sup>12</sup> and in nanoscale constrictions in superfluid <sup>3</sup>He.<sup>13</sup> Because they result in a doubly-degenerate phase potential when incorporated into a superconducting loop,  $\pi$  junctions have been proposed as building blocks for superconducting qubits.<sup>14</sup>

In this paper, we present measurements of the current-phase relation (CPR) of a SFS Josephson junction that demonstrate directly the sign change in the critical current when the junction undergoes a crossover into a  $\pi$  state below a temperature  $T_\pi$  at which the critical current vanishes. We also carefully investigate the crossover region near  $T_\pi$  to search for a  $\sin(2\phi)$  component in the CPR. This would be evidence for second-order Josephson coupling, which has been predicted to dominate in this region<sup>15-20</sup> and has been suggested by period doubling in the magnetic field modulation of the critical current of SFS arrays<sup>21</sup> and SNS SQUIDs.<sup>22</sup> We find no evidence for any  $\sin(2\phi)$  component.

A  $\pi$  junction is a Josephson junction with a negative critical current  $I_c$ . Thus, the current  $I_J$  through a  $\pi$  junction for a given superconducting phase difference across the junction  $\phi$ , assuming a purely sinusoidal form for the CPR, is given

by  $I_J(\phi) = -|I_c| \sin \phi = |I_c| \sin(\phi + \pi)$ , in terms of the magnitude of the critical current  $|I_c|$ . The minimum energy state of an isolated  $\pi$  junction corresponds to a phase shift of  $\pi$  across the junction,<sup>23</sup> in contrast to an ordinary Josephson junction, or 0-junction, for which the minimum energy is at zero phase difference.

In SF bilayer structures, superconducting correlations are known to exist in the F-layer due to the proximity effect. Because of the exchange field energy  $E_{\text{ex}}$ , Cooper pairs in the F-layer have nonzero center-of-mass momentum  $Q = 2E_{\text{ex}}/\hbar v_F$ , where  $v_F$  is the Fermi velocity. The wave function of these Cooper pairs at distance  $x$  from the SF interface obtains a phase multiplier  $\exp(+iQx)$  or  $\exp(-iQx)$ , depending on the orientation of the electron spins. Taking into account all spin states, the OP  $\Psi$  induced in the F-layer, has the form:

$$\Psi(x) \sim \cos\left(\frac{x}{\xi_{F2}}\right) \exp\left(-\frac{x}{\xi_{F1}}\right), \quad (1)$$

which describes the decay of the OP in the ferromagnetic layer over length  $\xi_{F1}$ , modulated by spatial oscillations with the period  $2\pi\xi_{F2}$ . In the dirty limit,  $\xi_{F1}$  and  $\xi_{F2}$  are given by:<sup>3</sup>

$$\xi_{F1, F2} = \left\{ \frac{\hbar D}{[(\pi k_B T)^2 + E_{\text{ex}}^2]^{1/2} \pm \pi k_B T} \right\}^{1/2}, \quad (2)$$

where  $D$  is the diffusion constant. Such oscillations of the OP have been confirmed in SF-bilayers by measurements of the superconducting critical temperature<sup>24</sup> and by tunneling spectroscopy.<sup>25</sup>

In SFS junctions, the OP oscillations cause the magnitude of the critical current to vary with the barrier thickness, vanishing at one or more thicknesses.<sup>4-6</sup> A ferromagnetic layer with thickness of order 1/2 (or other odd half-integer value) of the oscillation wavelength results in a sign change in the OP between the superconductor electrodes, meaning that the junction becomes a  $\pi$  junction. Although this condition can be achieved with ultrathin barriers of a strong ferromagnet,<sup>6</sup>

it is experimentally advantageous to use thicker barriers of a weakly-ferromagnetic alloy. Ferromagnetic layers with thicknesses in the range 10–30 nm are ideal because they are thick enough to form a uniform Josephson barrier yet thin enough to allow a measurable supercurrent. For  $\xi_{F1}$  and  $\xi_{F2}$  to be in the appropriate range, the Curie temperature of the ferromagnetic material should be of order 20–100 K. SFS  $\pi$  junctions of this type have been fabricated using metallic alloys consisting of the strong ferromagnet Ni diluted with either diamagnetic Cu (Ref. 3) or paramagnetic Pd.<sup>4</sup>

As can be seen from Eq. (2), both  $\xi_{F1}$  and  $\xi_{F2}$ , and hence the junction critical current, vary with temperature. Another advantage of a weak-ferromagnetic barrier is that  $E_{ex}$  can be made comparable to  $k_B T$  in the experimentally-accessible temperature range (1–4 K) so that the changes in  $\xi_{F1}$  and  $\xi_{F2}$  are maximized. This allows an SFS Josephson junction of appropriate barrier thickness to be tuned between the 0 and  $\pi$  states via temperature, enabling the crossover region to be explored in a single junction. We utilize this capability in our experiments.

Our SFS junctions were prepared in a multistep process by optical lithography and magnetron sputtering. The base and top superconducting layers are dc-sputtered Nb with thicknesses 100 nm and 240 nm, respectively, separated by a 22 nm barrier layer of rf-sputtered  $\text{Cu}_{0.47}\text{Ni}_{0.53}$ , a weakly-ferromagnetic alloy which has a Curie temperature of  $\sim 60$  K. The size of the junctions was  $50 \mu\text{m} \times 50 \mu\text{m}$ , as defined by a window in an insulating SiO layer deposited directly on top of the CuNi.

Because of the low normal state resistance of the SFS junctions ( $R_N \sim 10 \mu\Omega$ ), the current-voltage characteristics of the SFS junctions are measured using a SQUID potentiometer setup. In Fig. 1(a), we show a typical  $I$  vs  $V$  curve from which the critical current is determined. From a series of these curves, the critical current is plotted as a function of temperature, as in Fig. 1(b). As the temperature is lowered from 4.2 K, the critical current decreases, vanishes at a temperature  $T_\pi = 2.75$  K, and then increases again. This re-entrance is consistent with a transition between 0 junction and  $\pi$  junction states.<sup>3,5</sup> At the maximum critical current  $\sim 10 \mu\text{A}$ , the product  $I_c R_N \approx 100$  pV.

Conventional measurements of the current-voltage characteristic of the junction are not sensitive to the sign of the critical current nor to the shape of the current-phase relation; only  $|I_c|$  can be determined. To verify  $\pi$  junction behavior, it is necessary to perform a phase sensitive measurement by including the junction in a multiply-connected geometry. The sign of the critical current can be detected in an rf SQUID configuration by shorting the electrodes of the junction with a superconducting loop. For sufficiently high inductance  $L$  (such that  $|\beta_L| = 2\pi|I_c|L/\Phi_0 \gg 1$ ), a loop containing a  $\pi$  junction in zero applied magnetic field will exhibit a spontaneous circulating current, generating a magnetic flux of  $(1/2)\Phi_0$  in the loop which can be detected by a SQUID magnetometer or Hall probe; for smaller inductance, such that  $|\beta_L| < 1$ , it is energetically favorable to flip the phase of the junction into its high energy state  $\phi=0$  in which there is no circulating current. Alternatively, the junction can be connected in parallel with a conventional Josephson junction to form a dc SQUID. In this case, a  $\pi$  junction is identified by a minimum

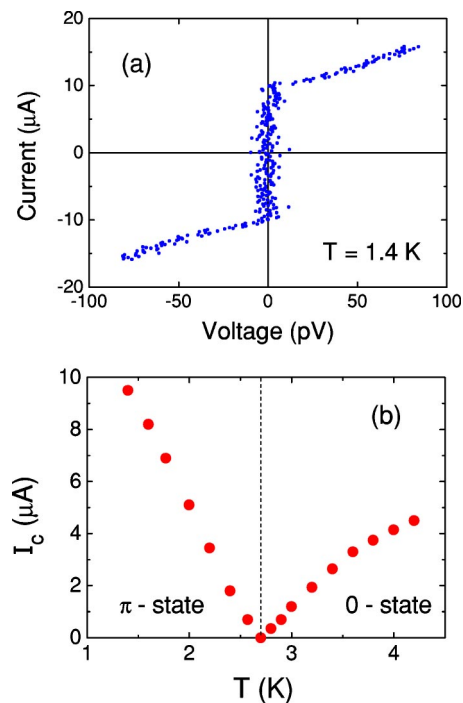


FIG. 1. (a) Current vs voltage for a Nb-CuNi-Nb Josephson junction measured at  $T=1.4$  K. (b) Variation of the critical current with temperature showing re-entrance at  $T \approx 2.7$  K characteristic of a transition into a  $\pi$  junction state.

of the SQUID critical current in zero magnetic field. We note that measurements of both the minimum in the critical current in dc corner SQUIDs (Ref. 26) and the spontaneous flux in tricrystal rings<sup>27</sup> have been used to demonstrate a similar but distinct effect, the phase shift of  $\pi$  between orthogonal directions in the  $d$ -wave superconducting cuprates.

The most complete way to characterize the  $\pi$ -junction behavior is to measure the current-phase relation (CPR). The CPR specifies the magnitude and sign of the sinusoidal component of the critical current as well as the amplitudes of any higher harmonics that may be present. The CPR can be measured in the rf SQUID configuration shown in Fig. 2(a). A dc SQUID galvanometer is used to measure the current  $I_L$  that flows through the superconducting loop as a function of the current  $I$  applied across the junction. The CPR function  $I_J(\phi)$  is related to  $I$  and  $I_L$  by

$$I = I_J(\phi) + I_L = I_J \left( \frac{2\pi\Phi}{\Phi_0} \right) + \frac{\Phi}{L}, \quad (3)$$

where  $\Phi$ , the total magnetic flux in the loop, is related to the junction phase  $\phi = 2\pi\Phi/\Phi_0$  by the phase constraint around the rf-SQUID loop, and to  $I_L = \Phi/L$  provided that there is no external flux linking the SQUID loop.

For our phase-sensitive measurements, the SFS  $\pi$  junction is incorporated into an rf-SQUID loop with inductance  $L \approx 1$  nH. This loop is fabricated in the shape of a planar washer which is coupled to a commercial dc SQUID sensor. As current  $I$  is applied across the SFS junction, the magnetic flux in the loop is modulated due to the winding of the phase of the Josephson junction according to Eq. (3). The induc-

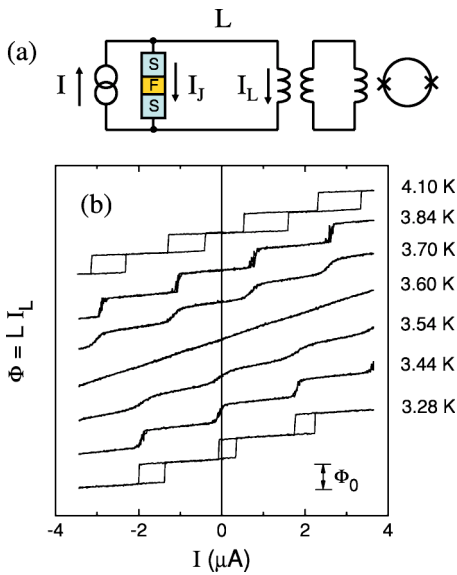


FIG. 2. (a) Circuit for measuring the current-phase relations of a SFS junction. (b) Magnetic flux  $\Phi$  in the rf SQUID loop vs applied current  $I$  showing a transition from hysteretic to nonhysteretic curves as  $|I_c|$  drops. Curves offset for clarity.

tance  $L$  determines the critical current range (here up to  $\sim 300$  nA) over which the rf-SQUID response remains nonhysteretic ( $|\beta_L| < 1$ ) so that the full CPR period can be mapped out.

For one sample, a series of curves plotting the flux in the rf-SQUID loop  $\Phi$  vs applied current  $I$  for different temperatures is shown in Fig. 2(b). We note that the flux axis is self-calibrating since each period corresponds to a one flux quantum  $\Phi_0$  change in the loop flux. Plotted in this form, the overall slope of the curves is  $L$ , the loop inductance, which is

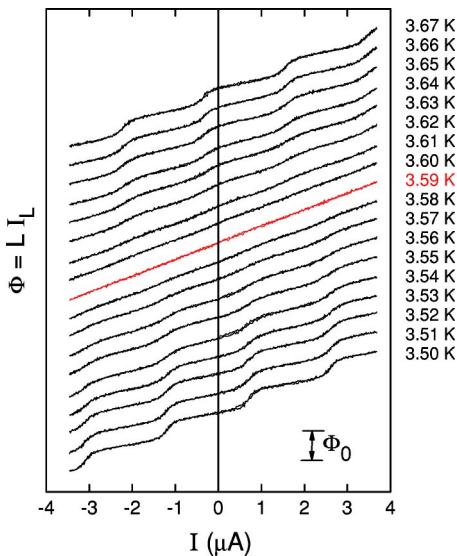


FIG. 3. Modulation of the magnetic flux in the rf SQUID loop as a function of current applied across the SFS junction for a series of temperatures. As the temperature is lowered, the critical current vanishes at  $T=3.59$  K, below which the modulation shifts phase by  $\pi$ . Curves offset for clarity.

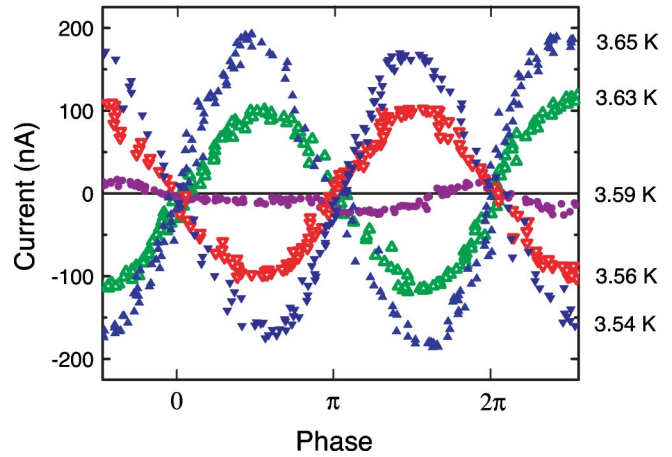


FIG. 4. Current-phase relation derived from the rf SQUID modulation curves of Fig. 3 showing the transition to a  $\pi$  Josephson junction as the temperature is lowered.

determined to be  $1.28 \pm 0.01$  nH. The curves are strongly hysteretic at  $T=4.2$  K and at low temperatures. They become nonhysteretic in the temperature range from 3.7 to 3.5 K. At  $T \approx 3.6$  K, there is no discernible modulation in  $\Phi$  indicating that  $I_c=0$ , and we identify this as the  $0-\pi$  junction crossover temperature  $T_\pi$ . All of the SFS junctions that we have studied were fabricated to exhibit a crossover temperature between  $0$  and  $\pi$ -states in the range  $2-4$  K.

Figure 3 shows in detail the temperature range for which  $-1 \leq \beta_L \leq 1$ . The modulation of the flux is now more accurately seen to disappear at  $T_\pi=3.59$  K. The most striking feature of the data in Figs. 2 and 3 is that the relative phase of the modulation abruptly changes by  $\pi$  as the temperature is varied from above to below  $T_\pi$ . Due to the presence of stray residual magnetic fields ( $\sim 10$  mG) in the cryostat, the phase of the modulation (and hence the junction phase difference) is not in general zero for zero applied current and varies slightly with temperature. This background phase shift is roughly linear in the vicinity of the  $0-\pi$  transition.

As can be seen in Eq. (3), the current-phase relation can be directly extracted from the data in Fig. 3 by subtracting

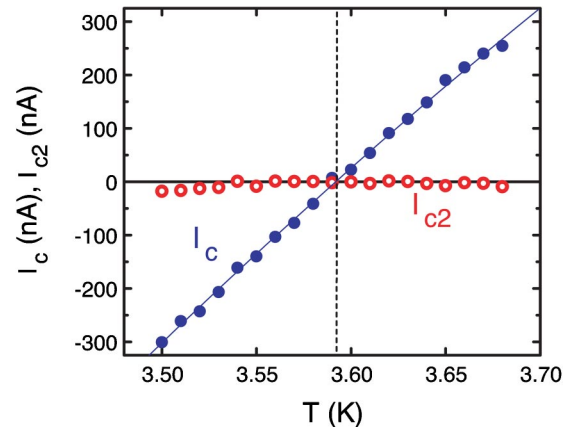


FIG. 5. Variation of  $I_c$  and  $I_{c2}$ , the  $\sin \phi$  and  $\sin(2\phi)$  components of the Josephson critical current, with temperature, showing the sign change in  $I_c$  and absence of a significant  $I_{c2}$ .

the linear flux term and taking account of any phase shifts arising from background fields. The CPR for several temperatures near  $T_\pi$  is shown in Fig. 4. The CPR has a sinusoidal form. No doubling of the periodicity is observed in the CPR at any temperature, suggesting that second-order Josephson tunneling harmonics, if present, never dominate the CPR of the junction. At  $T_\pi=3.59$  K, only aperiodic fluctuations of the current are observed, which limit the resolution of our critical current measurements to  $\sim 10$  nA. The CPR curves for temperatures above and below  $T_\pi=3.59$  K are out of phase by  $\pi$ , verifying that the critical current of the SFS Josephson junction changes sign at  $T_\pi$ .

The critical current as a function of temperature can be extracted from the CPR curves, or, more accurately, directly from the family of curves in Fig. 3 by fitting them to the form of Eq. (3). For the CPR, we assume the functional form  $I_f(\phi)=I_c \sin(\phi)+I_{c2} \sin(2\phi)$ , allowing for a second-order Josephson component.  $I_c$  and  $I_{c2}$  determined from the fits are plotted in Fig. 5. The temperature variation and sign change of  $I_c$  are clearly seen.  $I_{c2}$  is relatively flat, never exceeding a few percent of the maximum sinusoidal component  $I_c$  and, more significantly, vanishes along with  $I_c$  at  $T_\pi$ . This suggests that any induced  $I_{c2}$  value is likely an artifact of the fitting procedure rather than a physical second-order Josephson component in the CPR.

The absence of any  $\sin(2\phi)$  component is a significant result. Such terms have been widely predicted to arise and dominate the CPR at the crossover point, inhibiting the critical current from vanishing completely at  $T_\pi$ , in all implementations of  $\pi$  junctions, particularly SFS (Refs. 16 and 17) and SNS (Ref. 19) junctions. Some models predict that the barrier must be in the clean limit for which  $\ell > \xi_{FR}$ , where  $\ell$

is the mean free path in the ferromagnetic barrier, for second-order Josephson tunneling to dominate the CPR near the  $0-\pi$  transition.<sup>18</sup> However, this regime is not easily accessible in SFS junctions due to magnetic scattering; e.g. in our junctions,  $\ell \sim 1$  nm.

In conclusion, we have performed phase-sensitive measurements on SFS Josephson junctions that exhibit a transition from a 0 state into a  $\pi$  state at a crossover temperature  $T_\pi$ . The current-phase relation of the junctions is mapped out as a function of temperature, demonstrating the vanishing of  $I_c$  at  $T_\pi$  and the sign change in the critical current at this temperature. No higher-order harmonics in the CPR are observed for these junctions.

*Note added in proof:* In this paper, we have analyzed our results assuming that the SFS junctions studied had a barrier thickness near the first transition between 0 and  $\pi$  states that occurs as the barrier increases, implying a crossover from a 0-state into a  $\pi$ -state as the temperature is lowered. Recent experiments suggest that we may, in fact, be at the second transition so that the  $\pi$ -state is the higher temperature phase. As discussed in the paper, residual magnetic fields and trapped magnetic flux can shift the CPR curves, making it difficult to identify the states even though the transition is unambiguously demonstrated.

We thank Marco Aprili and Alexander Golubov for useful discussions. Work supported by the National Science Foundation Grant No. EIA-01-21568 and by the U.S. Civilian Research and Development Foundation (CRDF) Grant No. RP1-2413-CG-02. We also acknowledge extensive use of the Microfabrication Facility of the Frederick Seitz Materials Research Laboratory at the University of Illinois at Urbana-Champaign.

- 
- <sup>1</sup>A. I. Buzdin, L. N. Bulaevskii, and S. Panjukov, JETP Lett. **35**, 178 (1982).
- <sup>2</sup>A. V. Veretennikov, V. V. Ryazanov, V. A. Oboznov, A. Y. Rusanov, V. A. Larkin, and J. Aarts, Physica B **284-288**, 495 (2000).
- <sup>3</sup>V. V. Ryazanov, V. A. Oboznov, A. Y. Rusanov, A. V. Veretennikov, A. A. Golubov, and J. Aarts, Phys. Rev. Lett. **86**, 2427 (2001x).
- <sup>4</sup>T. Kontos, M. Aprili, J. Lesueur, F. Genet, B. Stephanidis, and R. Boursier, Phys. Rev. Lett. **89**, 137007 (2002).
- <sup>5</sup>H. Sellier, C. Baraduc, F. Lefloch, and R. Calemczuk, Phys. Rev. B **68**, 054531 (2003).
- <sup>6</sup>Y. Blum, A. Tsukernik, M. Karpovski, and A. Palevski, Phys. Rev. Lett. **89**, 187004 (2002).
- <sup>7</sup>V. V. Ryazanov, V. A. Oboznov, A. V. Veretennikov, and A. Y. Rusanov, Phys. Rev. B **65**, 020501(R) (2001).
- <sup>8</sup>W. Guichard, M. Aprili, O. Bourgeois, T. Kontos, J. Lesueur, and P. Gandit, Phys. Rev. Lett. **90**, 167001 (2003).
- <sup>9</sup>A. Bauer, J. Bentner, M. Aprili, M. L. Della Rocca, M. Reinwald, W. Wegscheider, and C. Strunk, Phys. Rev. Lett. **92**, 217001 (2004).
- <sup>10</sup>J. J. A. Baselmans, A. F. Morpurgo, B. J. van Wees, and T. M. Klapwijk, Nature (London) **397**, 43 (1999).
- <sup>11</sup>J. Huang, F. Pierre, T. T. Heikkilä, F. K. Wilhelm, and N. O. Birge, Phys. Rev. B **66**, 020507 (2002).
- <sup>12</sup>G. Testa, A. Monaco, E. Esposito, E. Sarnelli, D.-J. Kang, E. Tarte, S. Mennema, and M. Blamire, cond-mat/0310727 (unpublished).
- <sup>13</sup>A. Marchenkov, R. W. Simmonds, S. Backhaus, A. Loshak, J. C. Davis, and R. E. Packard, Phys. Rev. Lett. **83**, 3860 (1999).
- <sup>14</sup>L. B. Ioffe, V. B. Geshkenbein, M. V. Feigelman, A. L. Fauchere, and G. Blatter, Nature (London) **398**, 679 (1999).
- <sup>15</sup>A. A. Golubov, M. Y. Kupriyanov, and Y. V. Fominov, JETP Lett. **75**, 588 (2002).
- <sup>16</sup>N. M. Chtchelkatchev, W. Belzig, Y. Y. Nazarov, and C. Bruder, JETP Lett. **74**, 323 (2001).
- <sup>17</sup>Z. Radovic, N. Lazarides, and N. Flytzanis, Phys. Rev. B **68**, 014501 (2003).
- <sup>18</sup>Z. Radovic, L. Dobrosavljevic-Grujic, and B. Vujicic, Phys. Rev. B **63**, 214512 (2001).
- <sup>19</sup>T. T. Heikkilä, F. K. Wilhelm, and G. Schön, Europhys. Lett. **51**, 434 (2000).
- <sup>20</sup>Y. S. Barash and I. V. Bobkova, Phys. Rev. B **65**, 144502 (2002).
- <sup>21</sup>V. V. Ryazanov, V. A. Oboznov, A. V. Timofeev, and V. V. Bolginov, Microelectron. Eng. **69**, 341 (2003).
- <sup>22</sup>J. J. A. Baselmans, T. T. Heikkilä, B. J. van Wees, and T. M. Klapwijk, Phys. Rev. Lett. **89**, 207002 (2002).
- <sup>23</sup>L. N. Bulaevskii, V. V. Kuzii, and A. A. Sobyenin, JETP Lett. **25**,

- 290 (1977).
- <sup>24</sup>J. S. Jiang, D. Davidovic, D. H. Reich, and C. L. Chien, Phys. Rev. Lett. **74**, 314 (1995).
- <sup>25</sup>T. Kontos, M. Aprili, J. Lesueur, and X. Grison, Phys. Rev. Lett. **86**, 304 (2001).
- <sup>26</sup>D. A. Wollman, D. J. Van Harlingen, W. C. Lee, D. M. Ginsberg, and A. J. Leggett, Phys. Rev. Lett. **71**, 2134 (1993).
- <sup>27</sup>C. C. Tsuei, J. R. Kirtley, C. C. Chi, L. S. Yu-Jahnes, A. Gupta, T. Shaw, J. Z. Sun, and M. B. Ketchen, Phys. Rev. Lett. **73**, 593 (1994).